Proceedings of the Combustion Institute 42 (2026) 106038

Contents lists available at ScienceDirect

Proceedings of the Combustion Institute

journal homepage: www.elsevier.com/locate/proci

Direct measurements of hydrogen–air flame quenching distances in a converging channel under various wall temperatures

Dongliang Liu [a,*], Yuriy Shoshin [a], Nijso Beishuizen [a,b], Jeroen van Oijen [a]

[a] Eindhoven University of Technology, Mechanical Engineering, Eindhoven, The Netherlands
[b] Royal NLR - Netherlands Aerospace Centre, Amsterdam, The Netherlands

ARTICLE INFO

Keywords:
Flame quenching distances
Hydrogen–air flame
Experimental method
Converging channel
Wall temperature effect
Combustion safety

ABSTRACT

Flame quenching distances are fundamental data for combustion safety. In this study, we systematically investigate the quenching distances of hydrogen–air flames, with a particular focus on the influence of wall temperature, which mimics the practical boundary conditions in burners but has been overlooked in previous studies. The experiment used a converging rectangular channel with an accurately controlled gap spacing. Flame propagation was observed using Schlieren imaging, and the wall temperature was systematically changed and maintained by placing the channel within a hot air co-flow column. The flame quenching distance was determined by analyzing the channel gap width at the location where the flame front ceased to propagate. Measurements were conducted over a wide range of equivalence ratios (0.4–2.0) and wall temperatures from 20 °C to 282 °C. At room temperature, the measured quenching distances show excellent quantitative agreement with historical data, with a minimum value of approximately 0.51 mm occurring slightly rich of stoichiometry. Increasing wall temperature consistently reduces the quenching distance across all equivalence ratios, shifting the minimum quenching distance to approximately 0.40 mm at the highest tested temperature. The absolute reduction is most pronounced for very lean and very rich mixtures. The measured data generally follow the theoretical scaling proposed by Spalding, with the square of the quenching distance decreasing linearly with wall temperature.

Novelty and significance statement: This study presents the first direct measurements of hydrogen–air flame quenching distances in a converging channel under systematically varied wall temperatures. Unlike prior work, which largely neglected wall temperature effects, this study quantitatively demonstrates that elevated wall temperature reduces quenching distance and qualitatively characterizes effects of equivalence ratio and wall temperature on quenching interface morphologies. By establishing wall temperature as a critical parameter governing hydrogen–air flame quenching, this study fills a key gap in combustion safety research. The findings provide quantitative and morphological benchmarks directly applicable to the design of hydrogen combustion systems operating under realistic elevated-temperature conditions, strengthening the physical foundation needed for safe hydrogen energy adoption.

1. Introduction

Hydrogen is recognized as a promising carbon-free energy carrier for future energy systems [1]. Despite its advantages, the use of hydrogen as a fuel introduces significant safety concerns [2]. One critical aspect in ensuring the safe design of hydrogen burners is an accurate knowledge of the flame quenching distance. This requirement is essential because hydrogen combustion differs from conventional gaseous fuels due to its very small quenching distance [3] and its tendency to shift the stabilization point [4], which can overheat the burner rim and raise safety risks. Therefore, a deeper understanding of hydrogen's quenching distance is essential for developing safe hydrogen-based combustion systems.

It is important to note that the definition of quenching distance varies depending on the research context. In researches focused on internal combustion engines or gas turbines, the quenching distance is typically defined as the stand-off distance between a cold wall and the flame front [5–7]. In contrast, within the context of combustion safety and flame arrester — which is the focus of the present work — quenching distance is treated as the maximum allowable gap width, through which a flame front cannot propagate.

* Corresponding author.
E-mail address: d.liu2@tue.nl (D. Liu).

https://doi.org/10.1016/j.proci.2026.106038
Received 14 March 2026; Accepted 5 June 2026
Available online 24 June 2026

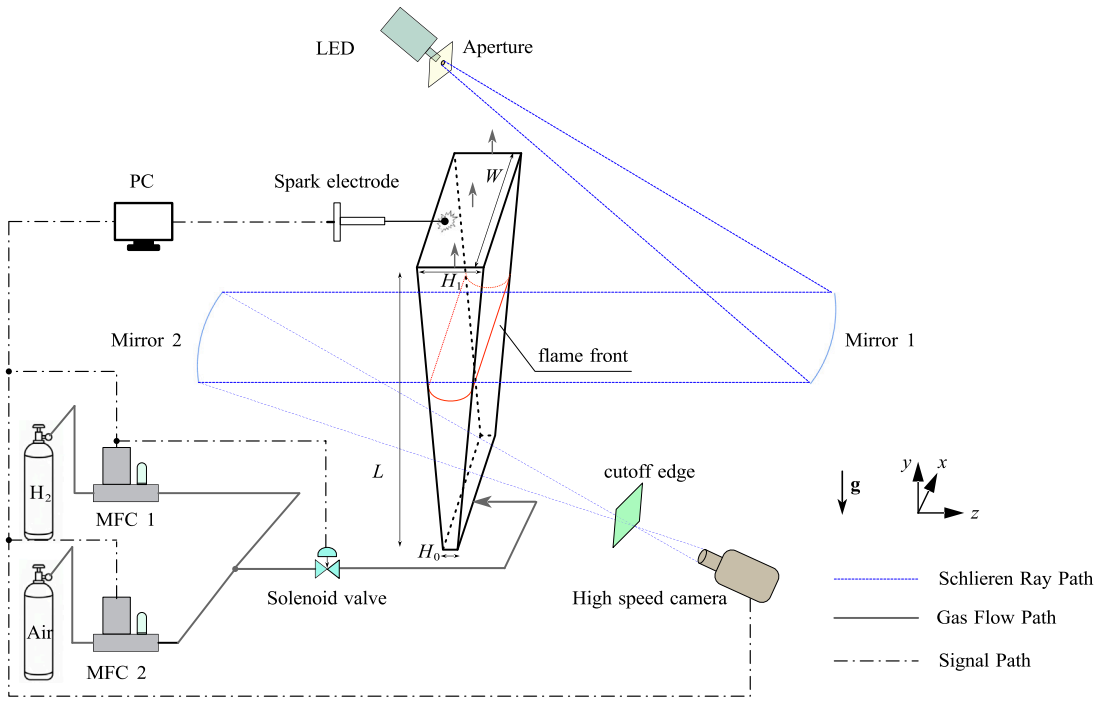

Fig. 1. Schematic diagram of the experimental apparatus for investigating flame quenching distances, which consists of three major systems: the combustion chamber with its gas supply system (solid gray lines), the control and data acquisition system (black dash-dotted lines), and the optical diagnostics system (blue dashed lines). All signal paths, including gas injection, spark timing, and data acquisition, are managed by a central PC.

Despite its importance, there are limited experimental observations regarding the quenching distance of the hydrogen flame. Potter and Berlad [8] measured hydrogen flame quenching distance using a slot burner inside a pressure-controlled chamber. They first establish a flame on the slot burner, then the hydrogen–air flow was interrupted using a simple shutoff valve. Researchers repeated this process to identify "critical points" that determines whether the flame is quenched or flashes back. Measurements were made for several slot widths (0.132, 0.213, and 0.323 mm), and the quenching distance was derived from these critical points. Jung et al. [3] measured hydrogen–air flame quenching distance using an annular stepwise diverging tube. Igniting the mixture (with an temperature of 296 ± 4 K) at the top, they let it travel downward into narrower gaps by adjusting the flow rate. An infrared camera tracked the flame position, allowing determination of the quenching distance from the gap size. Lewis and von Elbe [9] measured the quenching distance of hydrogen flame using the so-called flanged-electrode method in a closed vessel with two parallel electrodes (flanged by glass plates). A hydrogen–oxygen–inert gas mixture was introduced into the experimental apparatus, with the electrode gap systematically adjusted to vary the distance between electrodes. For each specific electrode spacing, the minimum spark energy required to achieve ignition was measured. It was observed that when the electrode separation was reduced below a certain threshold, ignition was no longer possible. This threshold spacing, representing the minimum distance at which flame initiation and subsequent propagation could still occur, was defined by the author as the quenching distance.

While the existing literature has established foundational knowledge regarding the quenching distance of hydrogen–air flames, the influence of wall temperature on the quenching distance has largely been overlooked. Since practical combustion systems often operate under elevated temperature boundary conditions, understanding how elevated wall temperatures impact the quenching distance is critical. Addressing this gap, the present work aims to directly observe and quantify the effect of wall temperature on hydrogen–air flame quenching in a converging channel, thereby providing new insights that are essential for the advancement of safe hydrogen combustion.

2. Experimental method

The main experimental apparatus used in this study is illustrated in Fig. 1. This setup was used for measurements conducted at room temperature, while the configuration used for higher-temperature measurements will be described later. The quenching distances were measured inside a vertically placed, converging rectangular channel, which was created by placing two quartz plates inside an aluminum channel and sealed from sides. One quartz plate is slightly inclined and pressed against the other, with precise spacers between them to accurately control the gap distance H_0. The overall channel length $L = 158$ mm, the channel width is $W = 67$ mm, the gap distance at the outlet is $H_1 = 4.20$ mm, and the gap distance at the inlet is $H_0 = 0.20$ mm.

Hydrogen gas, with a purity exceeding 99.99%, and compressed air, compliant with ISO 8573-1: 5-4-1 standards, were supplied through separate lines, with their flows individually controlled by mass flow controllers (MFCs). The hydrogen and air were premixed before being directed to a solenoid valve. After the valve, the mixture entered a plenum chamber designed to distribute the flow from the gas tubing into the wider quenching channel, after which it left the experimental setup.

The experiment procedure began with flushing the combustion chamber with hydrogen–air mixture of desired equivalence ratios for 40 s at a volumetric flow rate of approximate 4 LPM, making sure that the chamber was properly filled with the intended mixture. Then the solenoid valve was closed, and the system waited for 800 ms before ignition. This waiting period was sufficient to ensure that the flow inside the channel became quiescent. The combustible mixture was then ignited inside the quenching channel near the open top end by a spark electrode, resulting in a flame front propagating downward from open end toward the closed end. Although all experiments in the present study were conducted with downward flame propagation, buoyancy effects on the reported quenching distances are considered negligible due to the narrow channel gap distance [10,11].

The behavior of the hydrogen–air flame during the propagation and quenching was visualized using Z-type Schlieren imaging technique

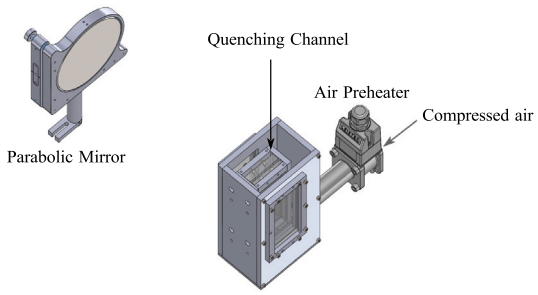

Fig. 2. Sketch of the heated setup. Compressed air was delivered to an air preheater, which regulates the outgoing air temperature. The heated air was then directed through the co-flow column, heating up the quenching channel.

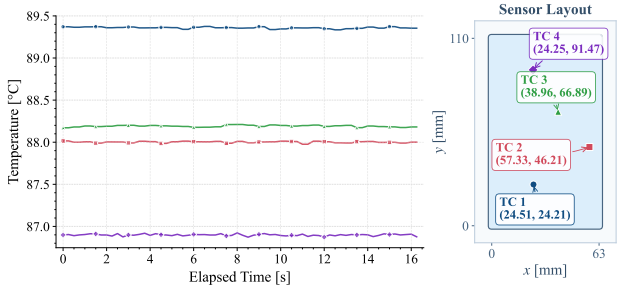

Fig. 3. Quenching channel temperature distribution and thermocouple location configuration. (Left) Measured temperature history for four independent thermocouples. (Right) Schematic of the sensor layout illustrating the location of the four thermocouples (TC 1–TC 4) across the field of view.

in conjunction with a high-speed camera. Light from an LED passed through an aperture and was collimated by parabolic mirror 1, with a focal length of 1200 mm and a diameter of 150 mm. The parallel rays passed through the test section, and were then refocused by an identical parabolic mirror 2. A horizontal knife edge acted as a cutoff plane, and the images were captured using a Photron Nova S6 high-speed camera at a frame rate of 9000 fps.

For the elevated wall temperature experiment, the entire quenching channel was placed inside a hot-air co-flow column, as shown in Fig. 2. To regulate the wall temperature during the experiments, a temperature controller was used to control the air preheater. The preheated air was then flushed through the co-flow column to maintain the desired wall temperature of the quenching channel. The uniformity of the wall temperature across the quartz plate was confirmed by recording temperature at sixteen randomly-selected locations (within the field of view). Fig. 3 presents the temperature history over an approximately 16-second interval of four thermocouples (TC 1–TC 4) that were attached directly to surface of the channel. With the target wall temperature set to 88 °C, these measurements confirm that the spatial temperature variation across the field of view remained tightly controlled at less than 3 °C.

It is important to note that the gas mixture temperature inside the channel is effectively equal to the wall temperature during flame propagation for two reasons. First, the hydrogen and air mixture undergoes preheating within the gas supply tubing. An additional 50 cm of gas tubing was coiled and positioned inside the hot air co-flow column, ensuring it maintained the same temperature as the quenching channel wall (T_w). Given flow rate of 4 LPM, the gas tubing geometry, the gas tube temperature, and the gas mixture inlet temperature (T_{in}), the gas outlet temperature (T_{out}) can be estimated using the energy balance for forced convection in a tube with constant wall temperature

$$T_{out} = T_w - (T_w - T_{in}) \exp\left(-\frac{hA_s}{\dot{m}c_p}\right),$$

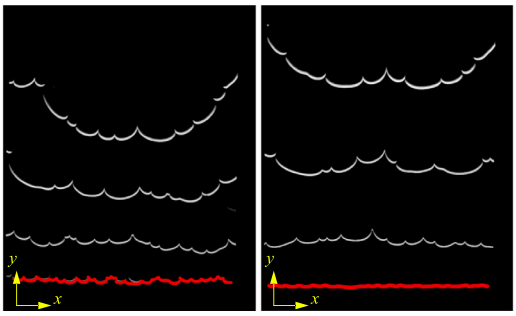

Fig. 4. A trajectory overlay of $\phi = 0.8$ and $\phi = 1.1$ flame propagation under room temperature of 20 °C. Throughout this process, the flame front is distinguished from the background as a sharp bright interface in the Schlieren images. Each successive flame position separated by a uniform time interval of 6.67 ms. The red line marks the quenching interface, where the flame propagation stopped.

where h is the average heat transfer coefficient, A_s is the total heat transfer area, $\dot{m}$ is the mass flow rate, and c_p is the specific heat of the mixture. Due to the high surface-area-to-mass-flow ratio of the 3 mm diameter gas tubing, the exponential decay term $\exp\left(-\frac{hA_s}{\dot{m}c_p}\right)$ becomes negligibly small (≈ 0), indicating that the outlet temperature effectively reaches the wall temperature. Second, upon entering the channel, the narrow geometry facilitates rapid heat dissipation, which maintains the gas temperature at the wall temperature. The characteristic heat conduction time, t_{cond}, is estimated as

$$t_{cond} = \frac{L^2}{\alpha},$$

where L is the channel gap width and α is the thermal diffusivity. Under the most conservative conditions in this study (maximum gap width and minimum thermal diffusivity), the maximum t_{cond} is 25 ms. This is significantly shorter than the 800 ms standby time prior to ignition, ensuring that the gas mixture reaches full thermal equilibrium with the channel walls.

3. Results and discussion

3.1. Quenching distance at room temperature

The flame propagation was monitored and the quenching was assessed at the location where the flame propagation stops. Fig. 4 depicts flame front trajectory for $\phi = 0.8$ and $\phi = 1.1$ flames, with each consecutive flame front position separated by a constant time step of $t = 6.67$ ms. As the hydrogen–air flame moves toward the narrower, closed end of the quenching channel, its propagation speed gradually decreases. The interface outlined by a red line is the location where the flame propagation ceased and the corresponding signal observed in the Schlieren image rapidly faded. Since the combustible mixture is quiescent during the flame propagation, the interface is therefore defined as the quenching interface. Both cases illustrate the characteristic development of wrinkled flame front separated by sharp cusps that dynamically emerge as the interface advances toward the quenching interface, which is consistent with established literature on flame wrinkling associated with various flame instabilities [12,13] or heat loss [14].

While both cases exhibit wrinkled flame development prior to reaching the quenching interface, the flame morphology is different during the quenching process. Fig. 5 gives a temporal stack of snapshots captured immediately before quenching. For the leaner case ($\phi = 0.8$), the wrinkled flame front approach the quenching location and extinguish abruptly. A representative instance of this extinction is highlighted by

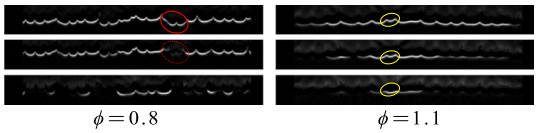

Fig. 5. Morphological comparison of the flame front near the quenching interface at room temperature. (Left) Sequential images showing quenching of a $\phi = 0.8$ flame. The red circle indicates a single flame cusp that quenches entirely. (Right) Snapshots of $\phi = 0.8$ flame quenching. The yellow circle marks a wrinkled flame structure that gradually flattens before quenching.

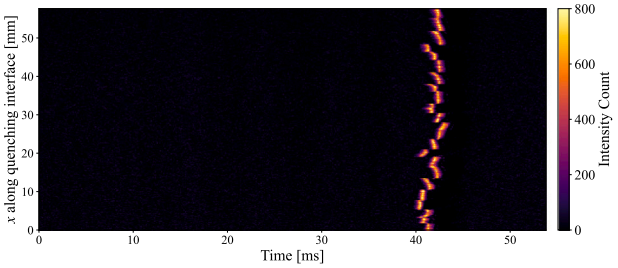

Fig. 6. The space–time intensity map (kymograph) along the quenching interface for $\phi = 0.8$ flame under room temperature. The intensity along x coordinate of the quenching interface, derived from the background-subtracted image, is plotted as a function of time. This plot illustrates the temporal evolution of pixel intensity along the quenching interface. The uneven bright band indicates the asynchronous arrival of different parts of the flame front at their quenching location, while the subsequent fading of intensity reveals the quenching that occurs after each piece of flame front has arrived.

the red circle. For the $\phi = 1.1$ flame, while it still has small wrinkled structures, the "amplitude" (the vertical height of the cusps) is much smaller than $\phi = 0.8$ flame. Furthermore, as these smaller structures approach the quenching location, the cusps visibly flatten (yellow circle). These distinct morphological behaviors result in a different final state: the $\phi = 0.8$ case produces a highly "rough" quenching interface, whereas the $\phi = 1.1$ case terminates at a nearly flat, weakly perturbed interface.

It is important to emphasize that the flame front does not reach the quenching interface simultaneously across the entire channel width. This asynchronous arrival is clearly illustrated in the space–time intensity map shown in Fig. 6. Before 39 ms, the dark void indicates that the flame front is still traveling and has not yet reached the quenching interface. At around 40 ms, bright spots begin to appear. Because the arriving front is wrinkled, the parts of the flame front that bulge forward hit the interface first, creating a distinct bright dot. As time continues, the rest of the curved flame front arrives at the quenching interface. Additionally, the narrow width of the bright band in the plot, which is about 1 ms, indicates that the quenching and subsequent heat dissipation occur very rapidly.

The gap width measured at the quenching interface directly represents the quenching distance for the flame under the specific equivalence ratio and wall temperature conditions. Fig. 7, for example, compares the spatial distribution and variation of the gap widths along the quenching interface under two different conditions ($\phi = 0.8$ and $\phi = 1.1$ flames). For the $\phi = 0.8$ flame, the "spiky" quenching interface gives a larger and more volatile gap widths, which fluctuate between 0.54 mm and 0.58 mm. The $\phi = 1.1$ flame, on the other hand, produces a smaller and more stable gap, which stay mostly between 0.50 mm and 0.52 mm. The inset histogram also shows how often specific gap widths occur throughout the quenching interface. For the $\phi = 1.1$ flame, the distribution is very narrow with a tall peak around 0.51 mm, which confirms high uniformity. For the $\phi = 0.8$ flame, the distribution is much wider and centered around 0.55 to 0.56 mm.

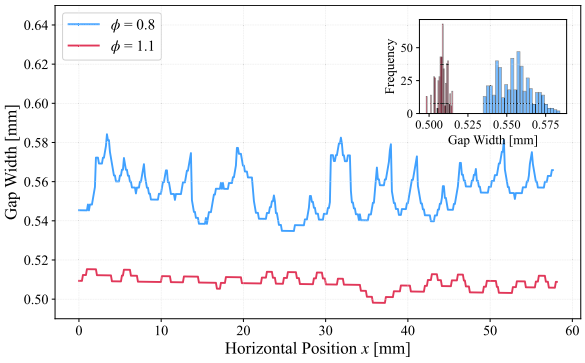

Fig. 7. Channel gap width at the quenching interface as a function of horizontal position for two conditions under 20 °C: $\phi = 0.8$ (blue) and $\phi = 1.1$ (red). The inset histogram displays the frequency distribution of gap width measurements for both conditions, highlighting the spread and central tendency of the gap width at the quenching interface.

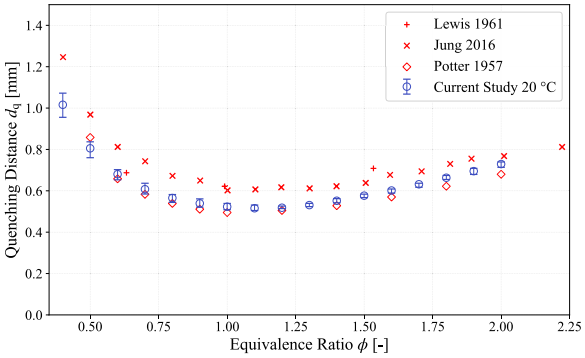

Fig. 8. Quenching distances of hydrogen–air flame under room temperature (20 °C). The upper error bar in the plot indicates the difference between the maximum and median quenching distances across the quenching interface, while the lower error bar represents the deviation between the minimum and median values.

The quenching distance can be statistically calculated as the median value from the distribution at the quenching interface, which is robust to extrema. A systematic examination of the quenching interface over a range of equivalence ratios revealed the measured quenching distance (d_q) as a function of the equivalence ratio at a wall temperature of 20 °C, as shown in Fig. 8. The minimum quenching distance of approximately 0.51 mm occurs slightly rich of stoichiometry ($\phi \approx 1.0 - 1.2$). The quenching distance increases sharply as the mixture approaches the limits of the equivalence ratio range considered in this study, particularly on the very lean side. The current experimental data demonstrate excellent quantitative agreement with the historical dataset of Potter [8] across the entire evaluated domain, as well as alignment with the limited data from Lewis and von Elbe [9]. However, while the data reported by Jung [3] exhibits an identical qualitative trend, it presents a systematic upward deviation of roughly 0.1 to 0.2 mm across all equivalence ratios. This consistent offset is likely a result of differences in experimental setup or boundary conditions rather than fundamental mixture properties. Overall, the current study shows a strong alignment with established literature.

The vertical error bar in Fig. 8 indicates the difference between median quenching distance and extrema. For near stoichiometric and rich flames, roughly between $\phi = 0.9$ and $\phi = 2.0$, the error bars are exceptionally small. In many cases, the difference is on the order of ±0.01 mm to ±0.02 mm, which indicates a high precision of the present study. However, for lean hydrogen–air mixtures, flame fronts

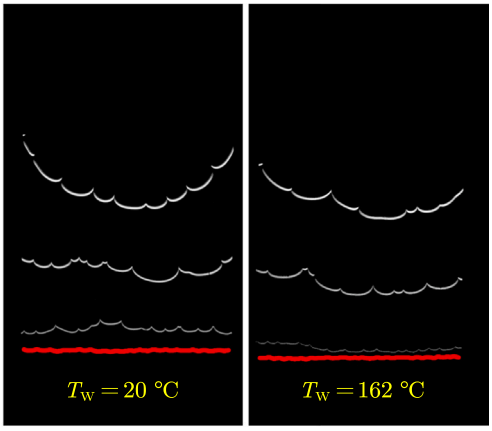

Fig. 9. Comparison of flame front trajectories for an equivalence ratio of $\phi = 1.1$. Consecutive snapshots are shown at time intervals of $t = 6.67$ ms (left) and $t = 4.44$ ms (right). The right curve indicates the quenching interface.

become more wrinkled, which results in the "rough" quenching interface. This physical instability inherently leads to higher scatter in the experimental measurements.

3.2. Quenching distance at elevated temperatures

Fig. 9 compares the flame front trajectories for $\phi = 1.1$ with two temperature settings. Obviously, for the elevated temperature case, the flame front penetrates deeper in the quenching channel than the room temperature case, leading to a smaller quenching distance.

In the left panel of Fig. 9, consecutive flame front positions are separated by a constant time interval of $t = 6.67$ ms, whereas in the right panel the interval is $t = 4.44$ ms. Despite the shorter sampling interval for the heated channel, the spatial separation between successive fronts in the right panel remains comparable to, or larger than, that in the left panel. This observation confirms that the flame propagates significantly faster in the heated channel. Furthermore, the increased wall temperature appears to suppress flame front wrinkling. The left panel displays a high frequency of small-scale wrinkled structures, while the right panel shows fewer and larger such structures.

In total, measurements at four elevated wall temperatures were taken (the unburnt mixture temperature is effectively the same as the wall temperature), and the results are given in Fig. 10. Overall, increasing the wall temperature consistently leads to a decrease in the median quenching distance for hydrogen–air flames across all tested equivalence ratios. The minimum quenching distance, which occurs slightly rich of stoichiometry, shifts from approximately 0.51 mm at room temperature to approximately 0.4 mm at the maximum tested temperature of 282 °C. Furthermore, a close examination shows that the absolute reduction in quenching distance is greater for extreme lean and rich flames than for near stoichiometric flames. For instance, at $\phi = 0.4$, the quenching distance drops from roughly 1.05 mm at 20 °C to 0.75 mm at 282 °C.

The observed decrease in quenching distance with increasing wall temperature generally aligns with the theoretical framework established by Spalding [15], even though the quenching distances for very lean mixtures exhibit greater scattering. In his analysis of flame quenching, Spalding incorporated a volumetric heat loss term into the energy equation. His findings showed that, when approaching quenching conditions and when pressure, mixture composition and the heat loss mechanism are unchanged, the quenching distance d_q is proportional to the square root of the difference between flame temperature and wall temperature:

$$d_q \propto \sqrt{T_f - T_w},$$

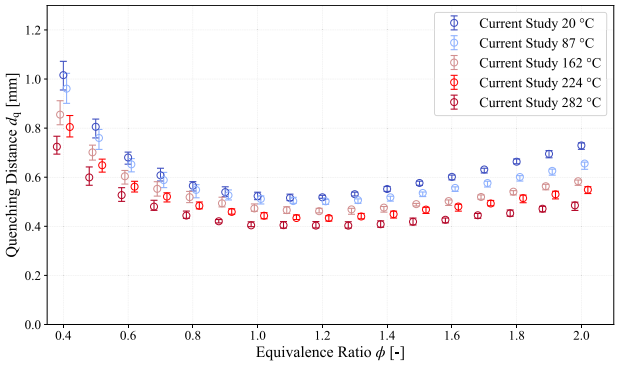

Fig. 10. Measured quenching distances for hydrogen–air flames at various wall temperatures. To improve data readability and prevent overlap of error bars, small artificial shifts were applied to the equivalence ratio values for elevated temperature sets: the 87 °C data were offset by +0.01, the 160 °C data by –0.01, the 228 °C data by +0.02, and the 282 °C data by –0.02. It is important to note that the data points for all temperatures were obtained at the same equivalence ratios.

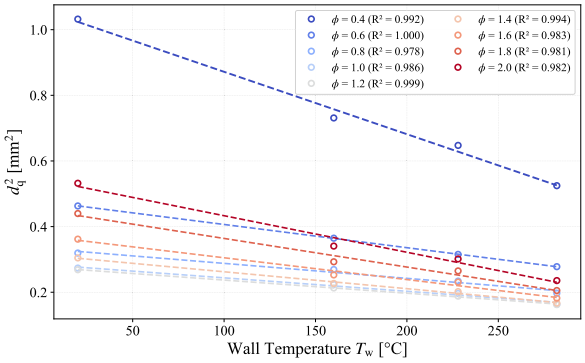

Fig. 11. Relationship between wall temperature T_w and the square of the quenching distance (d_q^2) for hydrogen–air flames at different equivalence ratios (ϕ). The dashed lines represent linear regression fits for each equivalence ratio. Values of the associated coefficient of determination R^2 are reported.

where T_f is the flame temperature and T_w is the wall temperature. Fig. 11 presents the relationship between the square of the measured quenching distance and the wall temperature. The results demonstrate that the experimental data generally follow the scaling law predicted by the theory. However, for very lean ($\phi = 0.4$) and very rich mixtures ($\phi = 1.8$ and 2.0), the data exhibit increased scatter around the fitted line. It should be noted that while Spalding's theoretical framework assumes a Lewis number of unity to simplify the analytical solution, the underlying quenching mechanism remains unaffected by this assumption. Consequently, the general phenomenological scaling holds.

4. Conclusion

This study presents the first direct observations and measurements of hydrogen–air flame quenching in a converging channel, with a focus on wall-temperature effects that are highly relevant to practical combustion systems but has received limited attention. The measurements performed at 20 °C are in good agreement with those reported in the literature, confirming the validity of the experimental setup. Moreover, a minimum quenching distance of approximately 0.51 mm is observed at a slightly rich equivalence ratio. The equivalence ratio also strongly affects the shape of the quenching interface. Lean flames tend to form a rough and highly disturbed quenching interface, while

near-stoichiometric and rich flames exhibit a smoother, flatter interface with fewer disturbances.

Increasing wall temperature consistently reduces the quenching distance across all investigated equivalence ratios (0.4–2.0), shifting the minimum value to approximately 0.40 mm at 282 °C, with the largest absolute reductions observed for very lean and very rich mixtures. The measured data generally follow Spalding's theoretical scaling, with the square of the quenching distance decreasing linearly with wall temperature. By systematically demonstrating hydrogen–air flame quenching distance with increasing wall temperature and various equivalence ratio, this study provides deeper insight into safe design and operation of hydrogen combustion systems under elevated wall temperature conditions.

CRediT authorship contribution statement

Dongliang Liu: Methodology, Investigation, Formal Analysis, Writing – original draft. **Yuriy Shoshin:** Methodology, Writing – review & editing, Supervision, Validation. **Nijso Beishuizen:** Conceptualization, Funding Acquisition, Supervision. **Jeroen van Oijen:** Conceptualization, Writing – review & editing, Supervision, Funding Acquisition, Validation.

Declaration of competing interest

The authors declare that they have no known competing financial interests or personal relationships that could have appeared to influence the work reported in this paper.

Acknowledgments

This project was funded by the Dutch Research Council (NWO), Netherlands under grant TKI HTSM/22.0024 (project VIPERS) and co-financed by Bosch Thermotechnology Deventer. The authors thank **Michel Cuijpers** (Eindhoven University of Technology) for managing lab support and logistics, and **Viktor Kornilov** (Eindhoven University of Technology) for technical suggestions.

References

[1] T. Capurso, M. Stefanizzi, M. Torresi, S.M. Camporeale, Perspective of the role of hydrogen in the 21st century energy transition, Energy Convers. Manage. 251 (2022) 114898.
[2] H. de Vries, H.B. Levinsky, Flashback, burning velocities and hydrogen admixture: Domestic appliance approval, gas regulation and appliance development, Appl. Energy 259 (2020) 114116.
[3] Y. Jung, M.J. Lee, N.I. Kim, Direct prediction of laminar burning velocity and quenching distance of hydrogen-air flames using an annular stepwise diverging tube (ASDT), Combust. Flame 164 (2016) 397–399.
[4] F.H. Vance, P. de Goey, J.A. van Oijen, The effect of thermal diffusion on stabilization of premixed flames, Combust. Flame 216 (2020) 45–57.
[5] A.O. Ojo, D. Escofet-Martin, C. Abram, B. Fond, B. Peterson, Precise surface temperature measurements at kHz-rates using phosphor thermometry to study flame-wall interactions in narrow passages, Combust. Flame 240 (2022) 111984.
[6] C. Jainski, M. Rißmann, B. Böhm, J. Janicka, A. Dreizler, Sidewall quenching of atmospheric laminar premixed flames studied by laser-based diagnostics, Combust. Flame 183 (2017) 271–282.
[7] H. Kosaka, F. Zentgraf, A. Scholtissek, L. Bischoff, T. Häber, R. Suntz, B. Albert, C. Hasse, A. Dreizler, Wall heat fluxes and CO formation/oxidation during laminar and turbulent side-wall quenching of methane and DME flames, Int. J. Heat Fluid Flow 70 (2018) 181–192.
[8] A.E. Potter, A.L. Berlad, The effect of fuel type and pressure on flame quenching, Symp. (Int.) Combust. 6 (1) (1957) 27–36.
[9] B. Lewis, G. von Elbe, Combustion waves in laminar flow, in: Combustion, Flames and Explosions of Gases (Second Edition), Academic Press, 1961, pp. 199–400.
[10] J. Jarosiński, Flame quenching by a cold wall, Combust. Flame 50 (1983) 167–175.
[11] J. Jarosinski, J. Podfilipski, T. Fodemski, Properties of flames propagating in propane-air mixtures near flammability and quenching limits, Combust. Sci. Technol. 174 (1) (2002) 167–187.
[12] L. Berger, K. Kleinheinz, A. Attili, H. Pitsch, Characteristic patterns of thermodiffusively unstable premixed lean hydrogen flames, Proc. Combust. Inst. 37 (2) (2019) 1879–1886.
[13] A.O. Ojo, D. Escofet-Martin, B. Peterson, High-precision 2D surface phosphor thermometry at kHz-rates during flame-wall interaction in narrow passages, Proc. Combust. Inst. 39 (1) (2023) 1455–1463.
[14] D. Martínez-Ruiz, F. Veiga-López, D. Fernández-Galisteo, V.N. Kurdyumov, M. Sánchez-Sanz, The role of conductive heat losses on the formation of isolated flame cells in Hele–Shaw chambers, Combust. Flame 209 (2019) 187–199.
[15] D.B. Spalding, A theory of inflammability limits and flame-quenching, Proc. R. Soc. A 240 (1220) (1957) 83–100.